

# Dolphin skin as a natural anisotropic compliant wall

V V Pavlov

Crimean State Medical University, Lenin blvd 5/7, Simferopol 95006, Ukraine

E-mail: [pavlovv@csmu.strace.net](mailto:pavlovv@csmu.strace.net)

Received 19 January 2006

Accepted for publication 13 June 2006

Published 10 July 2006

Online at [stacks.iop.org/BB/1/31](http://stacks.iop.org/BB/1/31)

## Abstract

Although the success of compliant walls in mimicking dolphin skin is well known, the drag-reducing properties of a dolphin's skin are still unclear. Moreover, little is known about the relation between the 3D structure of the skin and the local flow conditions. To study the role of a dolphin's skin in reducing the drag the skin morphology parameters were compared with the parameters of an anisotropic compliant wall and a possible flow–skin interface was considered. The 3D structure of skin from different locations was modelled using serial histological sections of the skin. The hydrodynamics of the dorsal fin of the harbour porpoise was studied by means of computer simulation of the flow around virtual models of the fin. It was found that the distribution of the skin morphology parameters is correlated with the local flow parameters on the fin surface. The skin structure appears to allow the flow–skin interface to behave similar to an anisotropic compliant wall in the regions of favourable and adverse pressure gradients on the fin. The relation founded between the skin morphology and the local flow parameters could be useful in the design of multipanel anisotropic compliant walls.

## 1. Introduction

Interest in the understanding of a dolphin's hydrodynamics was initiated by Sir J Gray who, in 1936, published his analysis of a dolphin's energetics, later called Gray's paradox. It was stated that by the assumed turbulent flow a dolphin should possess either enormously powerful muscles (seven times more power per unit mass than any other mammalian) or must be capable of maintaining the laminar flow by some extraordinary means. In the late 1950s the aerodynamicist Max Kramer claimed that a dolphin ensured a low level of friction drag by maintaining the laminar flow over most parts of its body. The dolphin's skin having an unusually ordered inner structure was considered to be a natural compliant wall effectively reducing the flow disturbances in the boundary layer (Kramer 1960a, 1960b). Kramer proposed the drag-reducing properties of a dolphin's skin as a solution of Gray's paradox and initiated numerous investigations of the structure and function both of dolphin skin and compliant walls.

Significantly more detailed data of different aspects of the morphology, physiology and swimming of dolphins are available now. The state-of-the-art view of dolphin hydrodynamics assumes a complex of adaptations, such as

an unsteady velocity and pressure gradients from accelerating water over the body, skin tension and microvibrations, shedding of the superficial layer of epidermis as well as skin damping, that provides the boundary layer stabilization in the swimming dolphin (Gray 1936, Haider and Lindsley 1964, Ridgway and Carder 1993, Babenko and Carpenter 2003, Romanenko 2002, Nagamine *et al* 2004). Considerable progress has also been achieved in the theory and practice of compliant walls and the current level of knowledge assumes a substantial postponement of the laminar-turbulent transition as well as a turbulent boundary layer stabilization by appropriately designed compliant walls (Gad-el-Hak 1996, Choi *et al* 1997, Carpenter *et al* 2000).

At present the paradox is that the initial question, whether a dolphin's skin reduces the drag, remains unresolved. Numerous accumulated data of the dolphin skin sometimes give a detailed picture of the skin morphology but do not explain the skin–flow interface (Parry 1949, Sokolov 1955, 1973, Sokolov *et al* 1971, Simpson and Gardner 1972, Spearman 1972, Palmer and Weddell 1964, Harrison and Thurley 1974, Stromberg 1989, Toedt *et al* 1997). Does it mean that the right conclusion based on erroneous assumption has been made?

Methodological problems of the experimental study of the boundary layer of the swimming dolphin are still a serious obstacle to answering this question. Unlike the classic experiments in hydromechanics (Gaster 1987), it is difficult to state a well-defined relation between the initial flow, skin properties and modified flow in the experimental study of the swimming dolphin (Hertel 1966, Pershin 1988, Fish and Rohr 1999, Romanenko 2002). The specificity of such a study is a variability of the flow parameters as well as the skin properties; the non-steady swimming of dolphins is combined with a changeable geometry of the body while morphology and mechanical properties of the skin can be altered by the tension of the skin muscle (Surkina 1971b, Babenko 1979). The bottleneck is the statement of the problem that could allow the reliable interpretation of the results obtained as direct evidence of the drag-reducing properties of a dolphin's skin.

The possible hydrodynamic function of a dolphin's skin (Babenko *et al* 1982) can be revealed indirectly by a comparison with the compliant wall. To this end the relation between the 3D structure of the skin and the local flow conditions on a harbour porpoise dorsal fin will be considered in the context of anisotropic compliant walls theory. This sort of compliant wall has a design that is most like the ordered dolphin's skin structure and possesses good drag-reducing properties (Carpenter and Morris 1990, Yeo 1990).

The approach used in this paper consists of the search for such conditions, where the relation between the flow parameters and the wall structure could be treated as unambiguous. To this end the dorsal fin of a dolphin was chosen and it was assumed that a dolphin swims rectilinearly with a constant velocity. As the shape of the dorsal fin as well as the skin structure is still invariable, its relation can be treated as unambiguous. It makes the wing-like dorsal fin of a dolphin a convenient model of the flow–skin interaction unlike the dolphin's body where the interface has a complex character. The dorsal fin looks like a more simple model where the potential drag-reducing properties of the skin are not masked by other effects. Comparison of the skin structure with anisotropic compliant wall parameters allows the interpretation of the local skin features from the point of view of the flow/wall interface.

## 2. Methods

Measurements were made on the dorsal fin of three harbour porpoises *Phocoena phocoena*, which were by-caught in a fishing net in Kalamita bay in Crimea, Black Sea in 1998. The fins were cut from the body and fixed in 10% neutral formalin. Eight cross sections of the fixed fins were made with equal intervals, % of span. A scheme of sampling representing a two-parameter mesh (8 cross sections, 20 points located in equal intervals along the cross section, as well as two points located at the same distance from the trailing edge,  $n = 192$ ) was used for the acquisition of the skin morphology and the flow parameters data (Pavlov 2003).

On the basis of the thickness measurements of the sections, a set of outlines of the fin cross sections was made. Then parametric models of the fins at a 1:1 scale were created

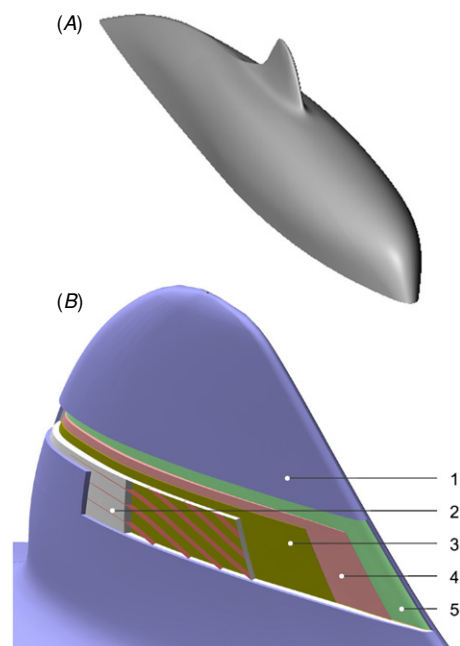


**Figure 1.** Modelling of the dorsal fin. (A) Combined model of harbour porpoise no 1. (B) 3D structure of the harbour porpoise no 2 dorsal fin. 1—the upper layer of the epidermis, 2—the papillary layer of the dermis, 3—the subpapillary layer of the dermis, 4—the ligamentous layer of the dermis, 5—core of the fin. Layers of the skin are removed from the centre of the fin to show the skin structure. A part of the papillary layer is shown without the epidermis and the number of the dermal ridges is reduced considerably in order to illustrate its arrangement. The epidermal septae between the dermal papillae as well as thickness of the dermal ridges are not modelled. The dermal ridges ending by dermal papillae are represented as ribbons.

with the SolidWorks software from SolidWorks Corp. In the model space, the  $X$ -axis corresponds to the streamwise direction, the  $Y$ -axis corresponds to the spanwise direction and the  $Z$ -axis corresponds to the direction normal to the fin planform. Additionally, a simplified model of the harbour porpoise body at a 1:1 scale was constructed on the basis of the body measurements and photos. The model presents the upper half of the body, with no flippers, flukes and complex details (eyes, blowhole). Each precise fin model was combined with a simplified body model in order to simulate natural conditions of the fin flow.

The hydrodynamic tests of the combined models (figure 1(A)) were done with the FloWorks software from Nika GmbH. Default turbulence and the boundary layer parameters are defined by FloWorks. The default boundary layer type (turbulent, laminar or transitional) is determined inside FloWorks from the Reynolds number defined on the equivalent hydraulic diameter  $D = 4A/P$ , where  $A$  is the opening cross section area and  $P$  is the perimeter of the opening. The layer thickness is determined from the effective wall length also governed by the Reynolds number. The default turbulence parameters are specified in terms of turbulent intensity (5%) and turbulent length (0.01 m). For most flows it is difficult to make a good estimation of the turbulence *a priori* so it is recommended that the default turbulence parameters be used.

**Table 1.** The characteristics of the computational domains used in this study. The project names NACA 0012 (1) and NACA 0012 (2) indicate the domains used for the validation of the FloWorks. The project names H porpoise nos 1–3 indicate the domains used for the study of the dorsal fin hydrodynamics.

Project name	$X_{\min}$ (m)	$X_{\max}$ (m)	$Y_{\min}$ (m)	$Y_{\max}$ (m)	$Z_{\min}$ (m)	$Z_{\max}$ (m)	Total cells	Fluid cells	Solid cells	Partial cells
NACA 0012 (1)	−0.247	1.045	−0.37	0.34	−0.1	0.1	377 184	342 528	26 272	8 384
NACA 0012 (2)	−0.247	1.045	−0.299	0.277	−0.025	0.025	294 476	258 062	30 856	5 558
H porpoise no 1	−0.385	0.286	−0.135	0.09	−0.025	0.025	519 666	291 417	135 002	93 247
H porpoise no 2	−0.383	0.289	−0.113	0.1	−0.025	0.025	462 476	251 075	129 081	82 320
H porpoise no 3	−0.384	0.28	−0.137	0.109	−0.03	0.03	469 126	263 434	114 669	91 023

To verify the FloWorks code the hydrodynamic tests of the NACA 0012 airfoil have been carried out. The NACA 0012 airfoil was chosen since it has long been a standard two-dimensional model for evaluating wind tunnel test techniques and evaluating methods (Abbot and von Doenhoff 1959, Harris 1981). Moreover, with some variability of the airfoil parameters, the cross sections of the dorsal fin of the harbour porpoise located near the fin base are similar to the NACA 0012 airfoil (Pavlov 2003).

The flow parameters of the airfoil were examined under the following conditions: chord length 0.635 m, wing span = 1 m, angle of attack  $\alpha = 3.66^\circ$ ,  $Re = 3 \times 10^6$ , Mach number  $M = 0.3$ . The characteristics of the computational domain are presented in table 1. The total number of cells of the orthogonal mesh of the computational domain is divided into the cells related to the fluid, the cells related to the solid and the cells that are partial, i.e. lying at the solid/fluid interface, partly in a fluid region and partly in a solid region. To estimate the effect of the size of the computational domain, the NACA 0012 airfoil was tested using two computational domains with different sizes (table 1).

The flow parameters were measured in 100 equally spaced (% chord) points along both the upper and lower surfaces of the airfoil. The chordwise pressure distribution was compared with the wind tunnel data of the NACA 0012 airfoil tested under the same conditions (Harris 1981). The pressure coefficient  $C_p$  was calculated as

$$C_p = \frac{P - P_\infty}{\frac{1}{2}\rho V_\infty^2},$$

where  $P$  is a local surface pressure,  $P_\infty$  is a free-stream pressure,  $\rho$  is the air density ( $1.225 \text{ kg m}^{-3}$ ) and  $V_\infty$  is a free-stream velocity.

The distribution of the averaged velocity, averaged pressure as well as the velocity vector at the boundary layer's outer boundary on the surface of the dorsal fin model was calculated using the following settings.

Analysis type—external. Result resolution—high (level 6). Geometry resolution—0.002 m. Physical features: heat transfer in solid—OFF; time settings—OFF; gravitation settings—OFF; compressibility effects—OFF; default wall conditions—adiabatic; fluid—water. Thermodynamic parameters: pressure—101325 Pa; temperature—20.05 °C. Velocity parameters:  $X$  component of velocity—8 m s<sup>−1</sup>;  $Y$  component of velocity—0 m s<sup>−1</sup>;  $Z$  component of velocity—0 m s<sup>−1</sup>. Turbulence parameters: turbulent intensity—5%; turbulent length—0.01 m. To obtain more accurate results, the

initial mesh density was increased significantly by specifying an advanced mesh option.

The angle  $\alpha$  formed by the dermal ridges with the  $Y$ -axis was used for the calculation of a 2D vector of dermal ridges. Then a 3D vector  $\mathbf{a}$  of the dermal ridges was obtained by the projection of the 2D vector on the surface of the 3D model (Pavlov 2003). The angle  $\beta$  formed by the dermal papillae with the  $Z$ -axis as well as the vector normal to the fin surface was used for the calculation of a 3D vector  $\mathbf{b}$  of the dermal papillae. Vectors  $\mathbf{a}$  and  $\mathbf{b}$  were used for the calculation of the local spatial orientation of the plane of the dermal ridges in the data points (figure 2(B)). Velocity vector  $\mathbf{c}$  at the same points on the fin surface was used for the calculation of the angle  $\varphi$  between the plane of the dermal ridges and a line corresponding to the local flow direction:

$$\sin \varphi = \left[ \frac{|(y_b \cdot z_a - z_b \cdot y_a)x_c + (x_b \cdot z_a - z_b \cdot x_a)y_c + (x_b \cdot y_a - y_b \cdot x_a)z_c|}{\sqrt{(y_b \cdot z_a - z_b \cdot y_a)^2 + (x_b \cdot z_a - z_b \cdot x_a)^2 + (x_b \cdot y_a - y_b \cdot x_a)^2}} \times \sqrt{(x_c^2 + y_c^2 + z_c^2)} \right],$$

where  $\mathbf{a}$  is the ridges vector,  $\mathbf{b}$  is the papillae vector and  $\mathbf{c}$  is the velocity vector.

The three-dimensional structure of the dermal–epidermal contact was examined at 33 data points on the fin in harbour porpoise no 2. Skin samples were cut into the serial 10  $\mu\text{m}$  histological sections in parallel to the skin surface. The numeration of sections begins from the first appearance of the dermal papillae (figure 6). The sections were stained by iron haematin. Images of scanned photographs of the sections were processed by the morphological filters and calibrated with Image-Pro software from Media Cybernetics. Processed 8 bit black-and-white images of the serial sections were used for the reconstruction of the dermis surface (figures 2(A), 6, 8(B)) with the IsoSurf software by Graham Treece. Specific volume  $V_v$ , as well as specific surface  $S_v$  of the papillary layer of the dermis with respect to a total height of the epidermis, was calculated.

The three-dimensional skin composition of the dorsal fin of harbour porpoise no 2 (figure 1(B)) was modelled using skin measurements made previously (Pavlov 2003).

A relation between the velocity distribution on the fin surface and angle  $\varphi$  as well as the parameters of the skin structure measured previously, such as the thickness of both

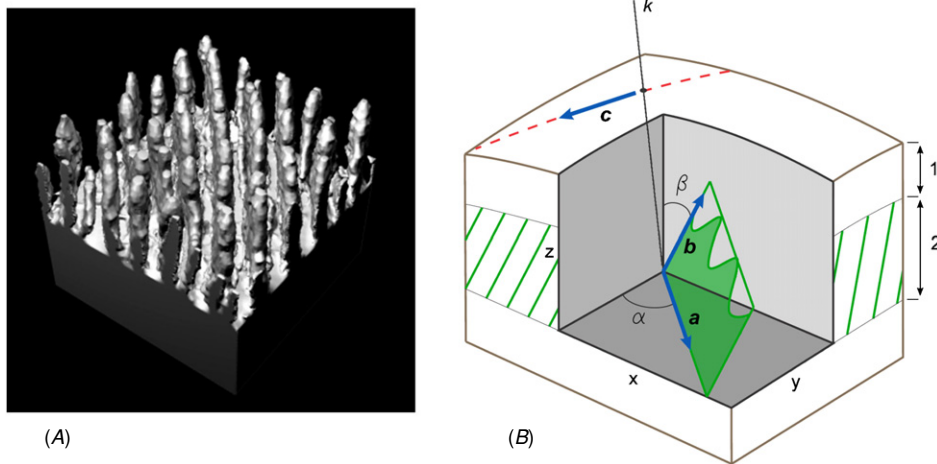


**Figure 2.** 3D structure of the skin. (A) 3D reconstruction of the papillary layer of the dermis. The planes of the dermal ridges ending with the dermal papillae are easily recognized. (B) A scheme of the basic measurements used for the calculation of the angle  $\varphi$ , see explanation in text. 1—the upper layer of the epidermis, 2—the papillary layer of the dermis.  $k$ —normal to the skin surface in the data point. The thicknesses of dermal ridges and dermal papillae are ignored. The dashed line indicates the local flow direction on the skin surface.

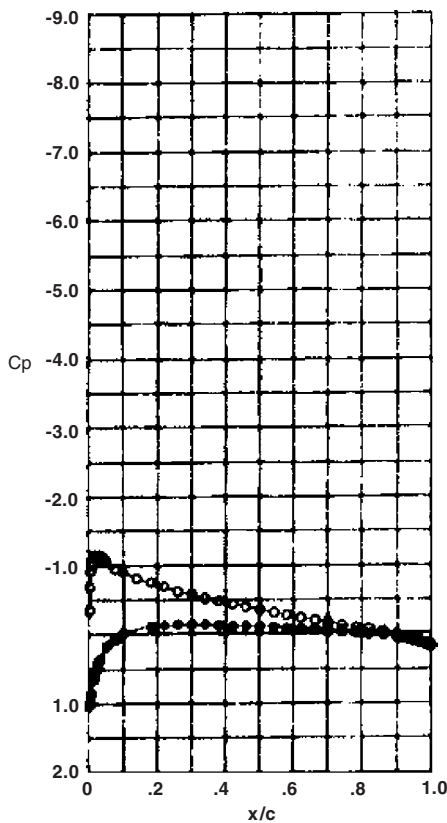


**Figure 3.** Wind tunnel data of the chordwise pressure distribution in NACA 0012 airfoil,  $C_p$ . (Reproduced from Harris (1981)). The upper line indicates the upper surface of the airfoil while the lower line indicates the lower surface.

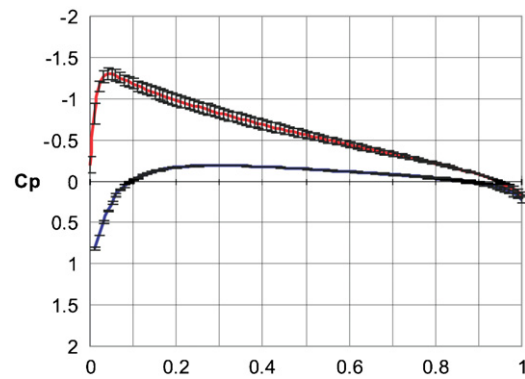


**Figure 4.** Chordwise pressure distribution in the NACA 0012 airfoil calculated using FloWorks,  $C_p \pm SD$ . The upper line indicates the upper surface of the airfoil while the lower line indicates the lower surface.

### 3. Results

#### 3.1. The FloWorks validation

The comparison of  $C_p$  based on the wind tunnel data (Harris 1981) with  $C_p$  calculated with the FloWorks revealed a similar pattern of the chordwise pressure distribution (figures 3 and 4). A subtle difference in the  $C_p$  values related to the different size of the computational domain was also revealed. As the goal of using FloWorks was to get a relative difference in hydrodynamic parameters of the fin flow rather than their exact values, it was assumed that FloWorks is valid for this study.

#### 3.2. Local variability of the dermal–epidermal contact

The pattern of the outer relief of the dermis varies significantly over the fin (figure 5). The dermis has no ridges at the narrow area (about 1 mm) along the leading edge from the fin tip to the fin base. There the shape of the dermal papillae is close

the upper layer of the epidermis and the papillary layer of the dermis (Pavlov 2003), was examined by a simple linear correlation.

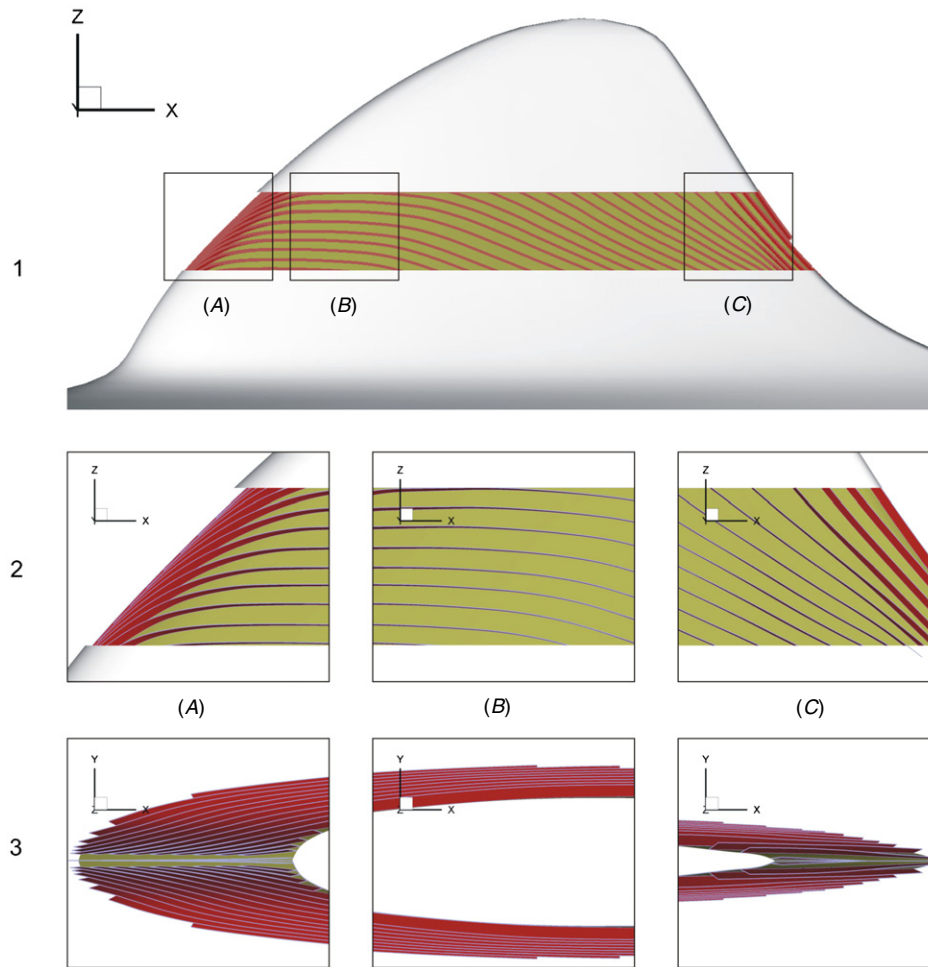


**Figure 5.** Orientation of the plane of the dermal ridges on the fin. 1—left view of the fin, 2—zoomed areas of the left view, 3—top view. (A) Near the leading edge, (B) at the PMT, (C) near the trailing edge. The epidermis is removed from the centre of the fin and the number of dermal ridges is reduced considerably for illustrative purpose.

to a cylindrical one. The dermal papillae are disconnected and no ordered pattern of their distribution is observed. The characteristic feature of the dermis near the leading edge is the relatively high dermal papillae that are approximately equal to the height of the dermal ridges. The higher density of the papillary layer of the dermis, i.e., a shorter distance between the dermal ridges also characterizes this area. There and on the fin planes the outer relief of the dermis is organized by the parallel dermal ridges ending with the dermal papillae that have a triangular form in the plane and are flattened in the orthogonal direction. Cross sections of the dermal papillae on the fin planes have an elongated elliptical shape. The height of the dermal papillae decreases smoothly from the leading edge to the trailing edge. Close to the trailing edge the dermal papillae almost disappear and merge with the dermal ridges.

The plane of the dermal ridges is rotated about the  $X$ -,  $Y$ - and  $Z$ -axes along the fin cross sections so that it virtually coincides with the  $XY$ -plane at the leading edge, with the  $ZX$ -plane at the position of maximal thickness (PMT) of the fin cross sections and with the  $XY$ -plane again at the trailing edge (figure 5).

Measurements of specific surface  $S_v$  and specific volume  $V_v$  of the papillary layer of the dermis show the relation of these parameters to the distance from the skin surface and also the position on the fin. Both parameters increase smoothly from the upper to the lower boundary of the papillary layer (figure 6). In addition, both parameters also increase along the fin cross sections from the leading to the trailing edge.

### 3.3. Hydrodynamics of the dorsal fin models

The velocity vector at the outer edge of the boundary layer on the dorsal fin surface changes its direction abruptly at the leading edge and then has almost a rectilinear direction until the location of the fast growth of the disturbances in the boundary layer near the trailing edge (figure 7(B)). The velocity has a steep positive gradient at the leading edge and then decreases to the trailing edge. There is a difference in the velocity distribution in the upper and lower parts of the fin. The velocity in the chordwise direction decreases gently over the upper part of the fin but more abruptly over the lower part (figure 7(A)).

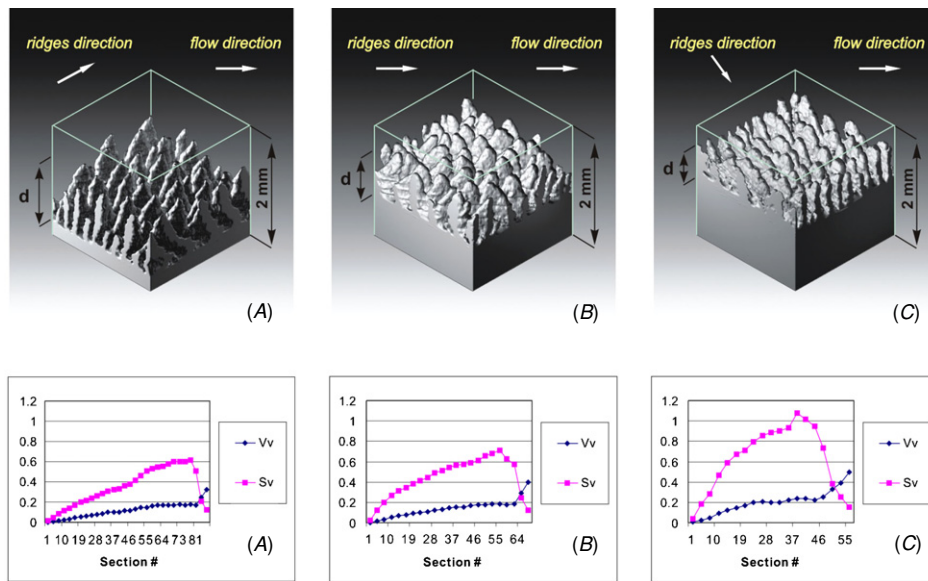


**Figure 6.** Differences in the 3D structure of the skin. The upper part of the figure shows the 3D reconstructions of the skin samples of equal volume located at different places along the cross section of the fin. (A) Near the leading edge, (B) at the PMT, (C) near the trailing edge. The epidermis is not shown. Letter  $d$  indicates the distance from the upper to the lower boundary of the papillary layer of the dermis. The lower part of the figure shows the increase of specific volume  $V_v$  as well as specific surface  $S_v$  of the dermis from the upper to the lower boundary of the papillary layer of the dermis.

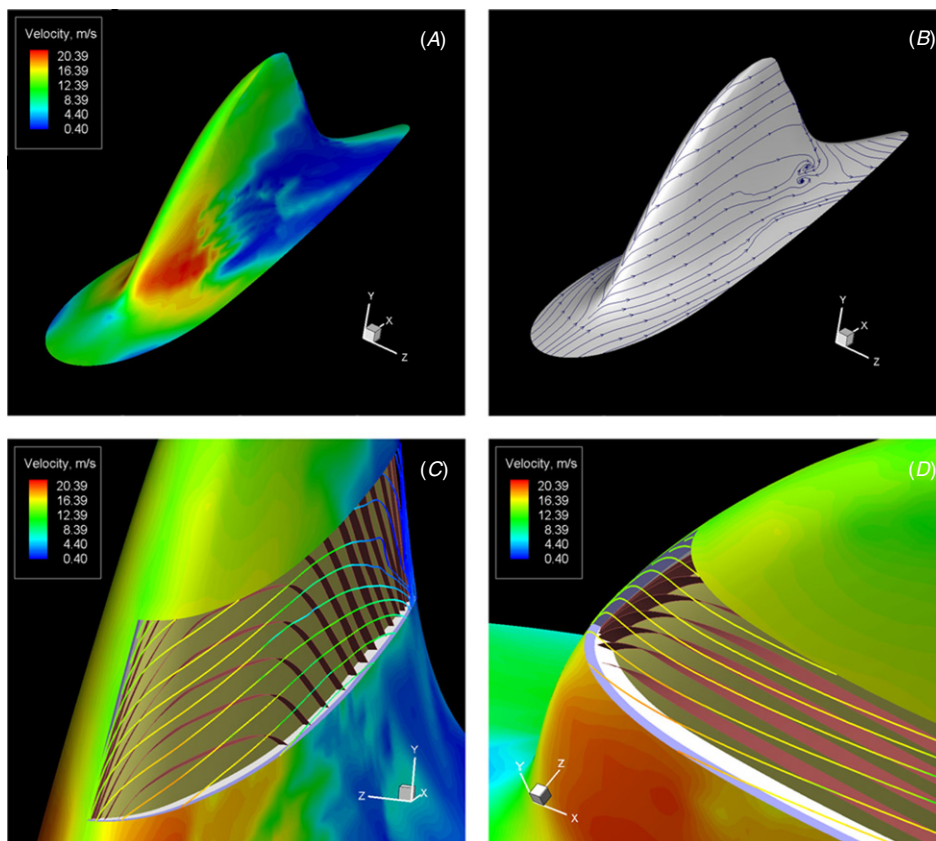


**Figure 7.** Hydrodynamics parameters of the dorsal fin. (A) Velocity distribution (harbour porpoise no 1), (B) velocity vector at the outer edge of the boundary layer on the dorsal fin surface (harbour porpoise no 1), (C)–(D) angle  $\varphi$  between the plane of the dermal ridges and velocity vector at the outer edge of the boundary layer on the dorsal fin surface (harbour porpoise no 2). The epidermis is removed from the centre of the fin and the number of dermal ridges is reduced considerably for illustrative purpose.

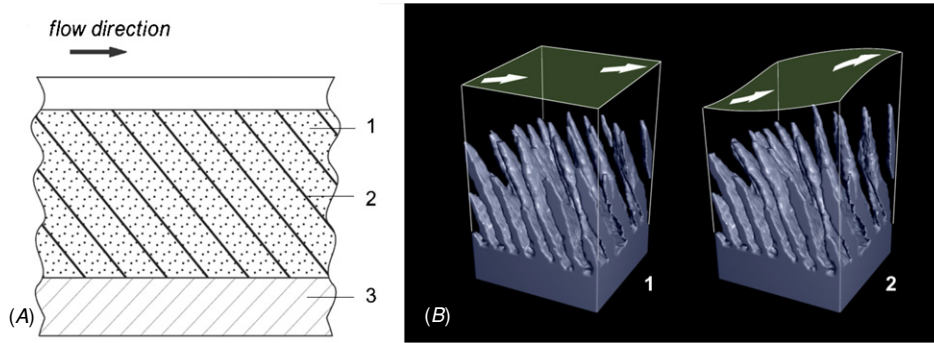


**Figure 8.** Compliant wall design and a dolphin's skin structure. (A) Sketch of a fibre-composite anisotropic compliant wall, redrawn from Carpenter and Morris (1990). 1—wall matrix, 2—aligned fibres, 3—rigid base. (B) Simulation of a dolphin's skin displacement under the shear stress. The arrows indicate the flow direction on the skin surface. The epidermis is not shown. 1—intact skin, 2—skin displacement.

**Table 2.** The correlation between the velocity and morphological parameters of the skin.

	H porpoise no 1			H porpoise no 2			H porpoise no 3		
	$r(X, Y)$	$p <$	$N$	$r(X, Y)$	$p <$	$N$	$r(X, Y)$	$p <$	$N$
ULE	0.39	0.01	192	0.45	0.01	192	0.31	0.01	192
DPL	0.44	0.01	192	0.28	0.01	192	0.49	0.01	192
$\varphi$	-0.32	0.01	192	-0.5	0.01	192	-0.05	0.47	192

All the models of the dorsal fin have an unstable flow near the trailing edge at the base of the fin. The leading edge of the fin has the highest level of pressure with the maximal values at the base of the fin. The steep negative pressure gradient near the leading edge reverses in the low pressure region; then the pressure grows again to the trailing edge. Over the upper part of the fin the pressure grows rapidly to the trailing edge, while the lower part has a more elongated low pressure region.

It was found that the skin structure parameters being of importance in the flow–skin interface correlate with the velocity distribution. The coefficients of the linear correlation between the velocity and thickness of the upper layer of the epidermis (ULE), the papillary layer of the dermis (DPL) and angle  $\varphi$  are presented in table 2.

## 4. Discussion

### 4.1. Dermal ridges

The ordered structure of the dermal–epidermal contact and the pattern of the dermal ridges orientation in cetaceans inspired suggestions of its possible relation with the flow direction. Sokolov (1955, 1973) describing the direction of the dermal ridges in different species assumed its possible hydrodynamic function. Palmer and Weddell (1964) describing the dermal ridges and the skin structure of a bottlenose dolphin suggested a specialized drag-reducing mechanism. Purves (1963, 1969) describing the direction of the dermal ridges in a common dolphin, harbour porpoise and false killer whale related the flow direction to the orientation of the dermal ridges in a dolphin's skin. Surkina (1971a, 1971b) made a detailed description of the direction of the dermal ridges on the body of a common dolphin. She measured the angle between the dermal ridges and a long axis of the body in eight locations and

assumed that the direction of dermal ridges can approximately indicate the flow direction over a dolphin's body. Sokolov *et al* (1968) carried out hydrodynamic tests on plasticine models of a harbour porpoise and a bottlenose dolphin. A certain resemblance was shown between the general arrangement of the dermal ridges and the ribbons indicating the flow direction around the models. Pavlov (2003) calculated the 3D vector of the dermal ridges direction in 192 data points on the dorsal fin of three harbour porpoises. It was shown that the direction of the dermal ridges is related to the calculated laminar, transition and turbulent flow of the fin. In all the mentioned studies the dermal ridges were considered as lines and no measurements of the angle between the dermal ridges and the flow direction were made.

Nevertheless, the dermal ridges as well as the dermal papillae in the skin of cetaceans have a 3D shape well described in the literature (Sokolov 1955, 1973, Naaktgeboren 1960, Stromberg 1989). In the general case these are the ridges of the dermis ending with the dermal papillae (figures 2(A), 6, 8(B)). The shape of the dermal ridges looks conservative, while the dermal papillae vary from a narrow cylindrical shape in a fin whale (Naaktgeboren 1960) to a 'flattened from both sides fir trees' shape in a bottlenose dolphin (Stromberg 1989). The laterally flattened shape of the dermal ridges and papillae can be represented by the plane that can be defined by two directions (figure 2(B)). First is the direction of the dermal ridges considered as the lines in publications mentioned above, while second is the inclination of the dermal papillae from the skin surface (Pershin 1988). Such a representation of the dermal ridges shape allows calculation of the angle between the 3D velocity vector over the non-planar surface of the skin and the plane of the dermal ridges within the papillary layer of dermis. It enables us to draw an analogy between a dolphin's skin structure and anisotropic compliant wall design.

#### 4.2. Compliant wall design and dolphin skin structure

The skin structure parameters correlate with the local flow parameters of the wing-like streamlined shape of the harbour porpoise dorsal fin. To answer the question of whether this correlation is a sign of the drag-reducing properties of a dolphin's skin, it is essential to consider the results obtained in the context of the compliant walls theory.

The frictional forces influence the flow of liquid close to the streamlined body. Due to viscosity the velocity of the flow increases from zero on the body surface to the free-stream velocity a short distance away. This region is called a boundary layer of fluid (Schlichting 1979).

The compliant wall suppresses the growth of instabilities in the boundary layer and achieves in excess of a fivefold delay in the laminar-to-turbulent flow transition as compared with a rigid wall (Dixon *et al* 1994). This effect as well as a favourably modulated turbulent boundary layer leads to the reduction of friction drag of the streamlined body.

A special kind of surface called an anisotropic compliant wall has an advantage of delaying transition in the boundary layer and of reducing the turbulence as well. In the general case, the wall matrix is reinforced by the aligned elements (fibres or voids) making the inner structure of the wall ordered (figure 8(A)). The structure of the anisotropic wall is arranged so that rather than being displaced up and down by the fluctuating pressure it is displaced in the direction making a substantial angle to the vertical, thereby generating a negative Reynolds shear stress on the compliant surface (Carpenter and Morris 1990). Such a response of the compliant wall suppresses the instability growth in the boundary layer reducing the shear stress level. The basic parameters of this kind of compliant wall are the angle formed by the fibres and the streamwise direction  $\Theta$ , elastic module  $E$ , inertial mass  $h\rho_m$ , where  $h$  is a wall thickness and  $\rho_m$  is a material density, and damping coefficient  $d$ . It was shown that with proper choice of  $E$  and  $\Theta$ , it might be possible to produce an anisotropic wall with a good potential for the drag reduction (Carpenter and Morris 1990, Yeo 1990).

The structure of a dolphin's skin has a similar design to the two-layer anisotropic compliant wall (Sokolov 1955, 1973, Palmer and Weddell 1964, Grosskreutz 1971, Stromberg 1989, Carpenter and Morris 1990, Yeo 1990). The epidermis reinforced by the dermal ridges reveals the skin anisotropy in the direction perpendicular to the dermal ridges (Sokolov *et al* 1971, Surkina 1971a). This composition makes possible the anisotropic wall behaviour of the skin in the case when the plane of the dermal ridges makes the angle with the flow direction. It allows the displacement of the upper layer of the skin in the direction making a substantial angle to the normal to the skin surface (figure 8(B)).

Unlike the fibre-composite compliant wall, the reinforcing elements of a dolphin's epidermis are the dermal ridges, arranged at an angle different to the flow direction. The angle  $\varphi$  formed by the plane of the dermal ridges with the flow direction can be considered as the analogue of  $\Theta$  in an anisotropic compliant wall. Other wall parameters such as  $E$ ,  $h\rho_m$  and  $d$  are related to the ratio of the thickness of the skin layers, specific volume of the vascular papillary layer and a

spatial density of the dermal ridges. Unlike  $\varphi$ , it cannot be calculated directly from the skin morphology parameters.

The cross sections of the harbour porpoise dorsal fin represent a well-studied hydrofoil shape (Abbot and von Doenhoff 1959, Lang 1966, Pershin 1975). The flow in the boundary layer along the hydrofoil develops from the laminar at the leading edge to the turbulent one near the PMT by the appropriate Reynolds number. Following the analogy with compliant walls it is of particular interest to consider the variability of  $\varphi$  correlated with the alteration of the flow parameters along the hydrofoil.

The curvature of the leading edge causes abrupt flow acceleration. The steep gradient of velocity indicates a high level of pressure and a shear stress load. At this location the dermal ridges make a positive angle with the flow direction, and  $\varphi$  varies rapidly from zero on the leading edge to the maximal values of  $45^\circ$ – $60^\circ$  over a short distance (figure 7(C)–(D)). The combination of the highest papillary layer, the specific shape of the dermal papillae and  $\varphi$  in the skin near the leading edge looks most appropriate for the skin displacement in the direction making a substantial angle to the normal to the skin surface. Here, the maximal values of  $\varphi$  are close to those of  $\Theta \pm 60$  in anisotropic compliant walls with the best performance in terms of transition delay (Carpenter and Morris 1990).

The PMT of the fin cross section indicates the transitional flow area over the rigid model of the fin. A zero or slightly positive adverse pressure gradient is inherent in this location. The plane of the dermal ridges is parallel to the flow direction and, consequently,  $\varphi = 0$  (figures 5(B), 7(C), (D)). Unlike the region close to the leading edge, such a structure of the skin indicates an absence of skin displacement similar to the behaviour of anisotropic compliant walls.

The skin near the trailing edge is mainly under the action of positive pressure gradient. Here the dermal ridges make a negative angle with the flow direction and  $\varphi$  increases from  $0^\circ$  to  $25^\circ$ – $45^\circ$ . The shape and low size of the dermal papillae as well as the lowest thickness of the epidermis and the papillary layer of the dermis (Pavlov 2003) indicate smaller skin displacement (figure 8(B)) in comparison with the area close to the leading edge.

The pattern of the flow–skin interface considered here has a general character. The flow along the fin cross section has spanwise variability on the dorsal fin. The fin base is under the influence of the developed turbulent boundary layer of a dolphin's body (Romanenko 2002), while the upper and the middle parts of the fin, apparently, have a combination of the laminar and transition modes of the boundary layer due to the low  $Re$  number of the fin cross sections. Therefore, the skin structure correlates with the flow characteristics related to the shape, e.g., with the negative and positive pressure gradients inherent to the flow of the hydrofoil rather than with laminar or turbulent mode of the boundary layer. On the other hand, the details of the flow–skin interface are still not as clear as other wall parameters, i.e.  $E$ ,  $h\rho_m$  and  $d$  remain unknown.

The rigid models used for the CFD simulation of the flow around the dorsal fin do not account for the compliance of the skin of the live dolphin. The results obtained can be considered

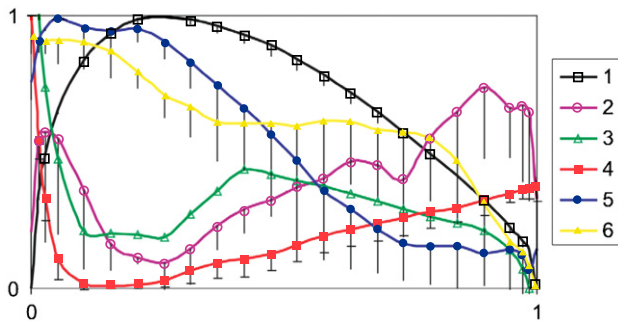


**Figure 9.** Variability of the flow and the skin structure parameters along the fin cross section taken at the middle of the fin. Data are normalized from 0 to 1. Bars indicate SD. 1—half of the cross section outline, 2— $\sin \varphi$ , 3—volume of the papillary layer of the dermis (H. porpoise no. 2), 4—pressure, 5—velocity, 6—height of the epidermis.

as a general idea of the flow around the fin as they can differ from those under natural conditions.

#### 4.3. Dolphin skin in hydrodynamic aspect

From the limited documented reports of the harbour porpoise swimming speed, the cruising speed was assumed as  $1.5\text{--}2\text{ m s}^{-1}$  while the burst speed was assumed as  $8\text{ m s}^{-1}$  (Fish and Rohr 1999). The skin on the dorsal fin of the harbour porpoise appears to be adapted well to the local flow conditions during a fast swimming. The skin morphology parameters correlate with the alteration of the velocity and pressure along the fin cross section (figure 9). The structure of the compliant skin of a dolphin appears to allow the displacement of the upper layer of the skin in the regions of favourable and adverse pressure gradients at the edges of the fin. This flow–skin interface behaves similar to anisotropic compliant walls and could suppress the instability growth in the boundary layer. The degree and direction of such a displacement can be controlled by the set of the skin morphology parameters (angle  $\varphi$ , ratio of the thickness of skin layers and spatial density of the dermal ridges) and differ in the regions of favourable and adverse pressure gradients.

The correlation of the skin features potentially important in flow stabilization with the local flow parameters corresponds well with the basics of compliant wall design. According to the principles of the structural and kinematical–dynamical interface of the flow/wall system (Babenko *et al* 1993), changes in the structure and properties of the compliant wall should correspond to the changes in the structure and properties of the disturbances in the boundary layer.

Following the analogy with Kramer’s studies the results obtained do not reveal the drag-reducing properties of a dolphin’s skin but leave us with a concept of the interesting design of a natural anisotropic compliant wall. Data obtained could be useful in the construction of the multi-panel compliant walls designed for the certain range of  $Re$  numbers where each section is adjusted to the local flow conditions (Carpenter 1993). In addition to the correlation founded between a spatial arrangement of reinforcing elements of the wall, i.e.

the dermal ridges, and the local flow, the proper values of  $E$ ,  $h\rho_m$  and  $d$  could be empirically selected using correlation founded (figure 9) between the flow parameters and the skin structure.

The possibility of the drag-reducing properties of the skin of a dolphin’s appendages is supported by a recent theoretical study by Allen and Bridges (2003). Investigation of the flow past a swept wing with a compliant surface established a stabilizing effect on the compliance on the boundary layer along the leading edge of the wing. A cetacean’s appendages increase the drag significantly (Lang and Pryor 1966, Yasui 1980). Despite the fact that appendages comprise only 12.4% of the total surface area of the harbour porpoise, however, they are responsible for 35.7% of the total drag (Yasui 1980). Given that, the friction drag of the wing-like well-streamlined appendages makes a considerable contribution to the total drag (Bushnell and Moore 1991), the adaptation of the skin to reduce the friction drag would decrease the swimming energy cost and, consequently, increase the survival value of animals (Videler 1995, Babenko and Carpenter 2003). In this respect the body surface adaptation to the boundary-layer dynamics in sharks is interesting. Unlike dolphin skin, the riblets on the shark’s scales are proven to be effective in reducing the friction drag (Bechert *et al* 1986). It was found that the shape of the scales depends on the position of the body with respect to the passing flow on a 2.55 m Galapagos shark *Carcharhinus galapagensis* (Bechert *et al* 1986). The pattern on the trunk is repeated across the pectoral fins. The adaptation directed to reducing friction drag on the appendages is apparently also important for the survival of the sharks as the large marine vertebrates.

The elegance of the natural solutions inspires new ideas in technology and engineering (Zhukovskii 1937, Fish 1998, Vincent and Mann 2002). A perfection of the drag-reducing adaptations of dolphins having been developed over about 50 millions years is worth investigating for the improvement of the performance of existing design in sea and air transports.

#### Acknowledgments

The author thanks P W Carpenter and V V Babenko for their valuable comments on the manuscript.

#### References

- Abbot I H and von Doenhoff A E 1959 *Theory of Wing Sections* (New York: Dover)
- Allen L and Bridges T J 2003 Flow past a swept wing with a compliant surface: stabilizing the attachment-line boundary layer *Stud. Appl. Math.* **110** 333–49
- Babenko V V 1979 Investigating the skin elasticity of live dolphins *Bionika* **13** 43–52 (in Russian)
- Babenko V V and Carpenter P W 2003 Dolphin hydrodynamics *Flow Past Highly Compliant Boundaries and in Collapsible Tubes* ed P W Carpenter and T J Pedley (Dordrecht: Kluwer) pp 293–323, chapter 13
- Babenko V V, Kanarskij M V and Korobov V I 1993 *Boundary Layer Over Elastic Surfaces* (Kiev: Naukova dumka) (in Russian)

- Babenko V V, Kozlov L F, Pershin S V, Sokolov V E and Tomilin A G 1982 Self-adjustment of skin dampening in cetaceans in active swimming *Bionika* **16** 3–10 (in Russian)
- Bechert D W, Bartenwerfer M, Hoppe G and Reif W E 1986 Drag reduction mechanisms derived from shark skin *AIAA 15th Congress of the Int. Council of the Aeronautical Sciences (London)* pp 1044–68
- Bushnell D M and Moore K J 1991 Drag reduction in nature *Ann. Rev. Fluid. Mech.* **23** 65–79
- Carpenter P W 1993 The optimization of multiple-panel compliant wall for delay of laminar-turbulence transition *AIAA J.* **31** 1187–8
- Carpenter P W, Davies C and Lucey A D 2000 Hydrodynamics and compliant walls: does the dolphin have a secret? *Curr. Sci.* **79** 758–65
- Carpenter P W and Morris P J 1990 The effect of anisotropic wall compliance on boundary-layer stability and transition *J. Fluid Mech.* **288** 171–223
- Choi K S, Yang X, Clayton B R, Glover E J, Atlar M, Semenov B N and Kulik V M 1997 Turbulent drag reduction using compliant surfaces *Proc. R. Soc. A* **453** 2229–40
- Dixon A E, Lucey A D and Carpenter P W 1994 The optimization of viscoelastic compliant walls for transition delay *AIAA J.* **32** 256–67
- Fish F E 1998 Imaginative solutions by marine organisms for drag reduction *Proc. Int. Symp. Seawater Drag Reduction (22–23 July, Newport, RI)* ed J C S Meng pp 443–50
- Fish F E and Rohr J J 1999 Review of dolphin hydrodynamics and swimming performance *SPAWARS System Center Technical Report 1801* (San Diego CA) p 196
- Gad-el-Hak M 1996 Compliant coatings: a decade of progress *Appl. Mech. Rev.* **49** 147–57
- Gaster M 1987 Is the dolphin a red herring? *Proc. IUTAM Symp. on Turbulent Management and Relaminarization (Bangalore)* (New York: Springer) pp 285–304
- Gray J 1936 Studies in animal locomotion VI the propulsive powers of the dolphin *J. Exp. Biol.* **13** 192–9
- Grosskreutz R 1971 Wechselwirkungen zwischen turbulenten Grenzschichten und weichen Wänden MPI für Stromungsforschung und der AVA *Göttingen Mitt* **53**
- Haider M and Lindsley D B 1964 Microvibrations in man and dolphin *Science* **146** 1181–3
- Harris C D 1981 Two-dimensional aerodynamic characteristics of the NACA0012 airfoil in the Langley 8-foot transonic pressure tunnel NASA TM 81927 p 137
- Harrison R J and Thurley K W 1974 Structure of the epidermis in tursiops, delphinus, orcinus and phocoena *Functional Anatomy of Marine Mammals* ed R J Harrison (London: Academic) pp 45–71
- Hertel H 1966 *Structure, Form and Movement* (New York: Rheinhold)
- Kramer M O 1960a Boundary layer stabilization by distributed damping *J. Am. Soc. Navig. Eng.* **72** 25–33
- Kramer M O 1960b The dolphin secret *New Sci.* **7** 1118–20
- Lang T G 1966 Hydrodynamic analysis of dolphin fin profiles *Nature* **209** 1110–1
- Lang T G and Pryor K 1966 Hydrodynamic performance of porpoises (*Stenella attenuata*) *Science* **152** 531–3
- Naaktgeboren C 1960 Die entwicklungsgeschichte der haut des finwals, *balaenoptera physalus* (L) *Zool. Anz.* **165** 159–67
- Nagamine H, Yamahata K, Hagiwara Y and Matsubara R 2004 Turbulence modification by compliant skin and strata-corneas desquamation of a swimming dolphin *J. Turb.* **18** 1–25
- Palmer E and Weddell G 1964 The relation between structure, innervation and function of the skin of the bottlenose dolphin (*Tursiops truncatus*) *Proc. Zool. Soc. Lond.* **143** 553–68
- Parry D A 1949 The structure of whale blubber, and a discussion of its thermal properties *Q. J. Micro. Sci.* **90** 13–25
- Pavlov V V 2003 Wing design and morphology of the harbour porpoise dorsal fin *J. Morphol.* **258** 284–95
- Pershin S V 1975 Hydrodynamic analysis of dolphin and whale fin profiles *Bionika* **9** 26–32 (in Russian)
- Pershin S V 1988 *Fundamentals of Hydrobionics* (Leningrad: Sudostroyeniye) p 264 (in Russian)
- Purves P E 1963 Locomotion in whales *Nature* **197** 334–7
- Purves P E 1969 The structure of the flukes in relation to laminar flow in cetaceans *Z. Saeugertier.* **34** 1–8
- Ridgway S H and Carder D A 1993 Features of dolphin skin with potential hydrodynamic importance *IEEE Eng. Med. Biol.* **12** 83–8
- Romanenko E V 2002 *Fish and Dolphin Swimming* (Sofia: Pensoft)
- Schlichting H 1979 *Boundary-Layer Theory* (New York: McGraw-Hill)
- Simpson J G and Gardner M B 1972 Comparative microscopic anatomy of selected marine mammals *Mammals of the Sea—Biology and Medicine* ed S H Ridgway (Springfield, IL: CC Thomas) pp 363–8
- Sokolov V E 1955 Structure of the integument of some cetaceans *Byulleten' Moskovskogo obshchestva Ispitatelej prirodi Otdel biologii* **60** 45–60 (in Russian)
- Sokolov V E 1973 *Integument of Mammals* (Moscow: Nauka) (in Russian)
- Sokolov V E, Kalashnikova M M and Rodionov V A 1971 Micro- and ultrastructure of the skin of harbour porpoise *Morphology and Ecology of Marine Mammals* ed V E Sokolov (Moscow: Nauka) pp 17–24 (in Russian)
- Sokolov V E, Kuznetsov G V and Rodionov V A 1968 The direction of the dermal ridges in dolphin skin in connection with peculiarity of the dolphin's body flow *Byulleten' Moskovskogo obshchestva Ispitatelej prirodi Otdel biologii* **73** 123–6 (in Russian)
- Spearman R I C 1972 The epidermal stratum corneum of the whale *J. Anat.* **113** 284–324
- Stromberg M W 1989 Dermal–epidermal relations in the skin of bottlenose dolphin (*Tursiops truncatus*) *Anat. Histol. Embryol.* **18** 1–13
- Surkina R M 1971a The distribution of dermal ridges over the body of a common dolphin *Bionika* **5** 88–94 (in Russian)
- Surkina R M 1971b Structure and function of the skin muscles of dolphins *Bionika* **5** 81–7 (in Russian)
- Toedt M E, Reuss L E, Dillaman R M and Pabst D A 1997 Collagen and elastin arrangement in the blubber of common dolphin (*Delphinus delphis*) *Am. Zool.* **37** 56A
- Videler J J 1995 Body surface adaptations to boundary layer dynamics *Biological Fluid Dynamics* ed C P Ellington and T J Pedley (Cambridge: Soc. Exp. Biol.) pp 1–20
- Vincent J F V and Mann D V 2002 Systematic technology transfer from biology to engineering *Phil. Trans. R. Soc. A* **360** 159–73
- Yasui W Y 1980 Morphometrics, hydrodynamics and energetics of locomotion for a small cetacean, *Phocoena phocoena* (L) MS Thesis University of Guelph, Ontario, Canada
- Yeo K S 1990 The hydrodynamic stability of boundary-layer flow over a class of anisotropic compliant walls *J. Fluid Mech.* **220** 125–60
- Zhukovskii N E 1937 To birds hovering *Complete works, V Vortices, Wing Theory, Aviation* (Moscow: Literature, Main Editorial Office of Aviation Literature) pp 7–35 (in Russian)